Open access • Journal Article • DOI:10.1038/S41566-017-0002-6

Ultrafast synthesis and switching of light polarization in nonlinear anisotropic metamaterials — Source link

Luke H. Nicholls, Francisco J. Rodríguez-Fortuño, Mazhar E. Nasir, R. Margoth Córdova-Castro ...+5 more authors

Institutions: King's College London, University of Sheffield, University of North Florida

Published on: 27 Sep 2017 - Nature Photonics (Nature Publishing Group)

Topics: Nonlinear optics, Metamaterial, Polarization (waves), Photonics and Anisotropy

DOI:
10.1038/s41566-017-0002-6

Document Version
Peer reviewed version

Ultrafast synthesis and switching of light polarization in nonlinear anisotropic metamaterials

Luke H. Nicholls[1], Francisco J. Rodríguez-Fortuño[1], Mazhar E. Nasir[1], R. Margoth Córdova-Castro[1], Nicolas Olivier[1]†, Gregory A. Wurtz[1]‡ & Anatoly V. Zayats[1]

[1]Department of Physics, King's College London, Strand, London WC2R 2LS, UK

†Present address: Department of Physics, The University of Sheffield, Sheffield, S10 2TN, UK

‡Present address: Department of Physics, University of North Florida, Jacksonville Florida 32224, USA

Optical communications, laser science, microscopy and metrology demand control of light polarization, also used as a probe of chemical and biological systems. Typically, certain polarization states of light are achieved using macroscopic anisotropic crystals. Metamaterials and metasurfaces have recently been developed to act as efficient passive polarization components of subwavelength dimensions[1-4], however active polarization control has so far been mainly limited to microwave and THz wavelengths[5-7]. Here we demonstrate all-optical switching of visible light polarization, achieving up to 60^o rotation of the polarization ellipse at picosecond timescales. This is accomplished both under control illumination and in a self-phase modulation regime, where the intensity of light affects its own polarization state, by exploiting the strong anisotropy and nonlinear response of a hyperbolic metamaterial[3,8-10]. The effects are general to any resonant, anisotropic, nonlinear nanoantennas and metasurfaces and suited to numerous photonic applications and material characterization techniques where ultrafast polarization shaping is required.

Active control and fast switching of the polarization state of light is required in many free-space and integrated photonics applications. In macroscopic optics, active control and modulation of light polarization is achieved by magneto-optical, in the case of Faraday rotators, or electro-optical, as with Pockels cells, effects. The latter provides arguably fastest switching rate, on nanosecond time scales, and is extensively used for signal encoding in telecommunications and for the development of ultrafast lasers, but is hardly suitable for integrated photonics applications. Recently, several implementations of metamaterials and metasurfaces have been developed to act as passive polarization components of subwavelength thickness. These include helical[1,11], split-ring-resonator-based[2,11-14] and hyperbolic metamaterials[3,15], as well as metasurfaces with chirality[16] and subwavelength phase control[4,17-19], but do not allow active control.

Metamaterials for active polarization components have been developed in the radiofrequency, microwave and THz spectral ranges, allowing for ease of fabrication, and have used a variety of modulation methods. These have included electrically tuneable pin-diode based elements[20,21], thermally controlled micro-cross metamaterials based on active semiconductor-metal phase changes [22], and mechanically deformable chiral materials capable of handedness switching of THz waves[23]. Coherent control of polarization has also been demonstrated in GHz metamaterials allowing enhancement or destruction of metamaterial polarization effects through counter-propagating beam interference[5]. In the THz spectral range, photo-induced conductivity changes in chiral metamaterials have been used to achieve up to 10^{o} polarization rotation with millisecond recovery times[6], while using optical excitation of wire-grid polarizers provided polarization modulation limited by a relaxation time of about 60 ps[7]. The ability to influence and tailor the polarization degree of freedom at THz switching rates has the potential to revolutionize many photonic applications and forge new techniques; for example, information on ultrafast chemical processes can be gained from

time resolved polarimetry. This fast switching can be achieved in metamaterials by exploiting free-electron nonlinearities of plasmonic metals induced by optical excitation, already demonstrated for strong light transmission modulation[9]. The all-optical control of polarization, where the polarization of a signal light pulse is controlled with another light pulse, may allow vastly improved switching rates, much higher than commercially available products.

Here, we use a strongly anisotropic nonlinear metamaterial based on a plasmonic gold nanorod array (Fig. 1), fabricated via self-assembly technique over large macroscopic areas, to demonstrate ultrafast all-optical switching of polarization of transmitted light: more than 60^{o} polarization rotation on sub-picosecond timescales, with switching rates of 0.3 THz calculated from the relaxation decay constant. Furthermore, intensity variations of the incident light can be encoded in its own polarization state upon transmission through the metamaterial. The effect is based on the different nonlinear phase changes experienced by the ordinary and extraordinary waves in the metamaterial and has a broadband nature with strongest polarization modulation near the effective plasma frequency of the metamaterial.

The changes to the polarization state of light transmitted through the anisotropic metamaterial were induced by illumination with femtosecond control light pulses (Fig. 1a). The incident polarized light ($\mathbf{E}_{inc}$) generally changes its polarization state upon transmission ($\mathbf{E}_{tx}$) through the anisotropic medium[24]. In the same way as conventional anisotropic materials, the nanorod metamaterial can be described by a permittivity tensor (See Supplementary Information) and supports ordinary (*o*-) waves, with electric field perpendicular to the nanorod axes, and extraordinary (*e*-) waves, with a component of the electric field along the nanorod axes, that experience generally different effective refractive indexes. In fact, one component of the permittivity tensor can be made to have an opposite sign to the others for wavelengths above the effective plasma frequency ω_{p}^{eff} of the

metamaterial, leading to strong anisotropic behaviour[3] (Supplementary Fig. 1). In this so-called hyperbolic regime, the metamaterial behaves as a transparent dielectric for light polarization normal to the principal axis and as a metal for light polarization along it[25]. This leads to extraordinarily high anisotropy not seen in nature, with Δn = 1.25-1.68 in a wavelength range 650-750 nm (Supplementary Fig. 1). Importantly, the *e-wave* has a resonance in transmission near the transition between the elliptic and the hyperbolic dispersion regimes. The following description of the effect would apply generally to any anisotropic material exhibiting a tunable resonance for one of the polarizations.

Under control light illumination, hyperbolic metamaterials exhibit a strongly enhanced Kerr-type optical nonlinearity near $\omega_{\mathrm{p}}^{\mathrm{eff}}$ [9,10]. This results in ultrafast light-induced variations of the ordinary (n_o) and extraordinary (n_e) refractive indices, due to changes in the electron temperature in the gold nanorods (see Supplementary Information). This nonlinearity influences ordinary and extraordinary refractive indices differently, allowing the use of control light of adjustable intensity to modulate transmitted signal light from its initial ground state output polarization $\mathbf{E}_{\mathrm{tx}}$ to a time-dependent excited state output polarization $\mathbf{E}'_{\mathrm{tx}}$, which can be expressed via Jones vectors[24] as

$$\mathbf{E}_{\mathrm{tx}} = \begin{pmatrix} t_o E^o_{\mathrm{inc}} \\ t_e E^e_{\mathrm{inc}} \end{pmatrix} \rightarrow \mathbf{E}'_{\mathrm{tx}} = \begin{pmatrix} t'_o E^o_{\mathrm{inc}} \\ t'_e E^e_{\mathrm{inc}} \end{pmatrix} \qquad (1)$$

where t_o and t_e are the transmission coefficients of the *o*- and *e*-waves, which act on the transverse magnetic (TM) and transverse electric (TE) polarization components of incident light respectively. The optical nonlinearities of the material induce a change in the coefficients $t_o \rightarrow t'_o$ and $t_e \rightarrow t'_e$. The situation is particularly interesting near the *e*-wave transmission resonance, as recent works have demonstrated that abrupt phase flipping near resonances are more sensitive than traditional transmission amplitude changes[26,27].

Under control light excitation, the *e*-wave resonance experiences a redshift[16], so that a wavelength range exists in which the phase of the transmission coefficient can be actively tuned between a '0-state' and a 'π-state' for the *e*-wave with little to no change in its amplitude, while keeping the same amplitude and phase for the *o*-wave ($t_o' \approx t_o$ and $t_e' \approx -t_e$, see schematic in Figure 1c). In this case, the polarization of a transmitted wave is modified from a ground state output ($E_{\mathrm{tx}}^o, E_{\mathrm{tx}}^e$), to an excited state output ($E_{\mathrm{tx}}^o, -E_{\mathrm{tx}}^e$) in the presence of control light illumination, i.e., "flipped" with respect to its *e*-component. This means that for transmitted linear polarizations with Jones vector $(1, \pm 1)$ and circular polarizations $(1, \pm \mathrm{i})$, one can achieve complete switching to their respective orthogonal polarizations $(1, \pm 1) \rightarrow (1, \mp 1)$ and $(1, \pm \mathrm{i}) \rightarrow (1, \mp \mathrm{i})$ upon control light illumination. This requires phase changes, and is not possible to achieve by modulating the output intensity of the ordinary and extraordinary components only. In practice, transmission coefficients may deviate slightly from this idealized behavior, so linear and circular polarizations at the output will be elliptical upon excitation. Fig. 1d shows experimentally measured optical properties of the fabricated nanorod metamaterial. The measurements exhibit a sharp resonance for the extraordinary waves at a wavelength of 698 nm for the ground state of the metamaterial, which, on excitation, red shifts to 705 nm. Thus, this uniaxial nonlinear crystal can be used for polarization synthesis based on nonlinear phase changes of ordinary and extraordinary waves near the metamaterial's effective plasma frequency. Note that the strong polarization change refers to different states of the output (transmitted) light, not to the polarization of input and output light. Near a broad resonance, output states have considerably lower amplitude than input states, as in the studied metamaterial, but increasing the sharpness of the resonance will allow the device to operate with both full phase shift and low insertion loss (the phase shift retrieved from the measurements is shown in Supplementary Fig. 2).

Furthermore, the observed effect could also be utilized in reflection, removing loss constraints experienced in transmission.

The transient transmission spectra (Fig. 2a), measured for different time delays Δt between a white light signal and a 585 nm control light femtosecond pulse, show negligible changes in optical density $\Delta OD(\Delta t) = OD(\Delta t) - OD(\Delta t < 0)$ for the ordinary wave in the spectral range of interest. Conversely, a strong red-shift, approximately 10 nm, of the transmission minimum of the extraordinary wave is observed near the effective plasma frequency, followed by a fast recovery with a 3.4 ps time constant (Fig. 2a and Supplementary Fig. 3). This red-shift of the *e*-wave resonance and the associated phase change described above, confirmed experimentally in Fig. 1d, lead to strong polarization changes of the transmitted signal light in the wavelength range near the effective plasma frequency.

The dynamics of four different polarization components of the transmitted signal light were measured (Fig. 2b) for both TE and TM polarizations corresponding to the ordinary and extraordinary transmitted waves with Jones vectors (1,0) and (0,1), respectively, and both diagonal linear polarizations (1,1) and (1, −1). Importantly, at each measured wavelength, quarter and half waveplates are used to tune the incident light polarization such that the transmitted light polarization is close to diagonal (1, −1) in the ground state by minimizing the (1,1) component. Therefore, the (1, −1) polarization component is labelled as co-polarized, and the (1,1) as cross-polarized. Under control light illumination, the transmitted intensity at a wavelength of 700 nm in the cross-polarized state increases three-fold (Fig. 2b). The effect is so dramatic that the cross- and co-polarized signals effectively swap intensity level upon control action. With careful optimization, high contrast on-off states can be achieved.

The transmitted polarization ellipse can be directly retrieved from the measured intensity of the four different linear polarization components (see Supplementary Information). Experimental measurements and numerical simulations of the polarization ellipse changes are in good agreement (Fig. 3a). Under control illumination, strong modulations of the polarization components at 700 nm are associated to rotations of the polarization ellipse of over 60^{o} (Figs. 3a,b,c). The polarization state then relaxes back to the ground state polarization. At the wavelengths to the red and to the blue of the effective plasma frequency, positive and negative rotation angles are observed, respectively. The experimental rotation angles agree with the expected values obtained from the simulations (Fig. 3c). The nonlinear effects not only modify the polarization ellipse orientation but also swap the handedness of the polarization of the transmitted light compared to the ground state in a given wavelength range (Fig. 3a and Supplementary Fig. 4).

The angle of rotation of the transmitted polarization state can be further controlled at a given wavelength by altering the power of the control light (Figs. 4a,d). This is due to the smaller phase changes obtained for decreased control intensities. Lower control intensity results in a smaller red-shift of the *e*-wave resonance of a finite width, where a larger red-shift is required to achieve a π phase shift for the broad resonance. Note that, in theory, interference effects can be used to achieve a metamaterial transmission coefficient that crosses exactly zero, even for lossy constituent materials, associated with an instantaneous π phase shift. In practice, imperfections and inhomogeneity will always result in a non-zero transmission at a resonance, associated with a finite bandwidth required for the phase shift.

A more complex mechanism of self-induced nonlinear polarization changes of the transmitted light can also be observed. If the incident signal light is strong enough, the leading front of the pulse induces electron-temperature-dependent changes of the permittivity which in addition to a phase shift may lead to self-induced transparency or absorption[10],

influencing the polarization state of the transmitted pulse as a whole (Figs. 4b,e). This self-action effect is relatively strong and produces a change in the orientation of the polarization ellipse of more than 60º. This opens a new degree of freedom for potential devices, where the polarization of light depends self-consistently on its intensity, and can be used for self-modulation and power limiting functionalities if observed through a polarizer. It should be noted that while the low power polarization state was recoverable after each measurement presented in Fig. 4, no recovery was observed when intensities over a damage threshold of 80 GW cm^{-2} were used. The working range of active polarization control can be tuned by designing a metamaterial with an effective plasma frequency in a required spectral range; to illustrate this, the self-action effect was also studied on a different sample, with ω_p^{eff} situated around 590 nm exhibiting similar behavior to other samples, as expected, although with slightly weaker experimental polarization ellipse rotations of about 25º (Figs. 4c,f).

In summary, we have shown that strong and ultrafast all-optical modulation of transmitted light polarization can be achieved in anisotropic nanorod metamaterials. This anisotropy was controlled with femtosecond light pulses leading to strong modulation of the intensity and a more than 60º rotation of the polarization state of a signal light pulse, 6 times larger than previous all-optical polarization control studies at THz wavelength[6] and at order of magnitude improved switching time[7]. The intensity of the incident light was used to control its polarization state through a self-modulation effect upon transmission through the metamaterial. We associate the high strength and efficiency of the polarization modulation to (i) the strong nonlinear optical response of the metamaterial and (ii) the use of abrupt phase changes near the effective plasma frequency of the metamaterial. The common approach of using changes in output intensity caused by resonance shifts usually results in relatively small differential changes, here we instead exploit abrupt phase changes to control the polarization state of a signal beam, an effect that easily translates into an intensity modulation through the

use of polarizing filters. This proposed ultrathin nonlinear device acts as a polarization switch at sub-picosecond speeds. Further studies into these effects and optimization could provide real promise in all-optical polarization control in integrated nanodevices at very high speeds. These nonlinear anisotropic metamaterials are fabricated using a scalable electrochemical approach over cm-size metamaterial chips and can be used in all possible photonic and laser science environments in the same way as conventional anisotropic and nonlinear crystals. Apart from ultrafast polarization modulation and coding, other applications based on the presented effect can be foreseen in high-resolution and single-molecule imaging; quantum information processing, where control and manipulation of the polarization states of light is extremely important, as well as sensing applications, where polarization adjustment and detection leads to improved refractive index sensitivities and possibly chiral molecule identification.

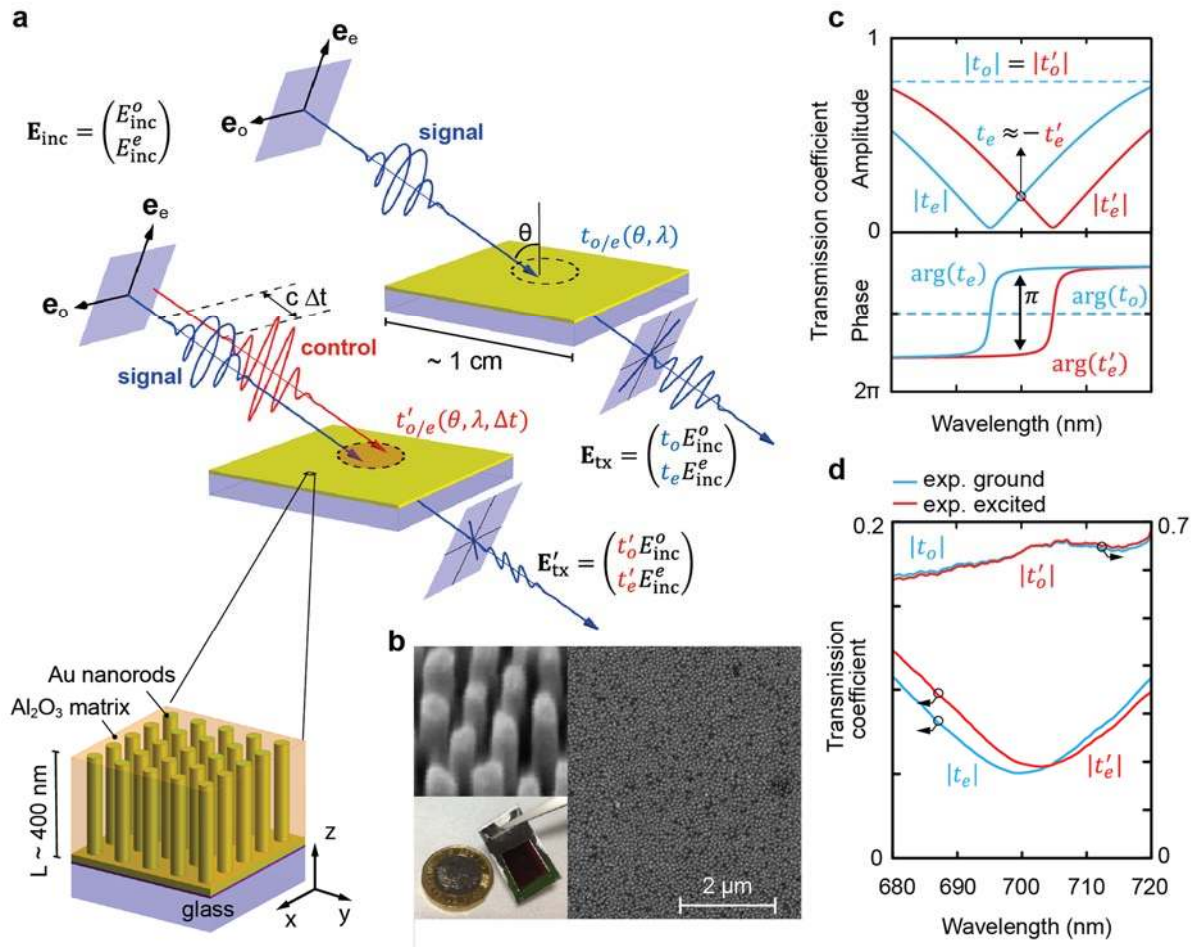

Fig. 1. **The principle of polarization synthesis with anisotropic metamaterial.** (**a**) Schematics of polarized light interaction with nanorod metamaterial in a pump-probe configuration. The control light modifies the anisotropy of the metamaterial which is probed by a time-delayed signal light. Inset: schematic of the metamaterial with Cartesian reference frame. (**b**) SEM image of the sample surface. Inset tilted image of a typical nanorod sample with the alumina template removed and photograph of the full sample area. (**c**) Illustration of the polarization modulation mechanism: due to a nonlinearity-induced shift of the resonance, a π phase shift can be experienced by the transmitted extraordinary wave with the ordinary wave unaffected. (**d**) Experimentally measured *o*- and *e*-wave transmission spectra for an angle of incidence $\theta = 45^{o}$ without (blue) and with (red) control light illumination.

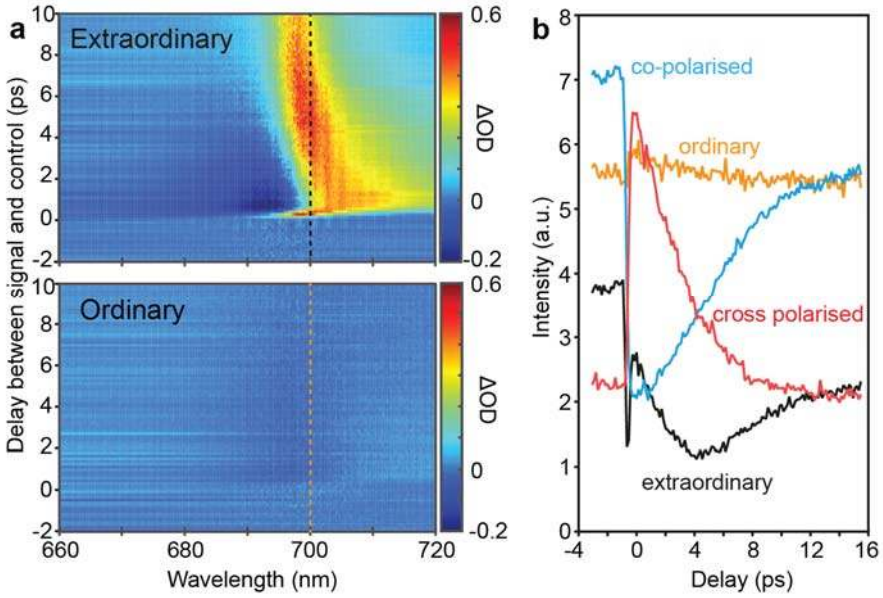

Fig. 2. **Polarized transmission dynamics.** (**a**) Transient spectra of changes in optical density (ΔOD) for extraordinary and ordinary waves through the metamaterial for an angle of incidence of $\theta = 45^{o}$. The incident light polarization was optimized to minimize the cross-polarized component at the output at 700 nm. Control light wavelength and peak power density are 585 nm and 16 GW cm^{-2}, respectively. The dashed line indicates cross-sections plotted in (b). (**b**) Transient transmission dynamics at a wavelength of 700 nm for selected output polarization components which are used to reconstruct polarization ellipses in Fig. 3 (cross-section indicated in (a)).

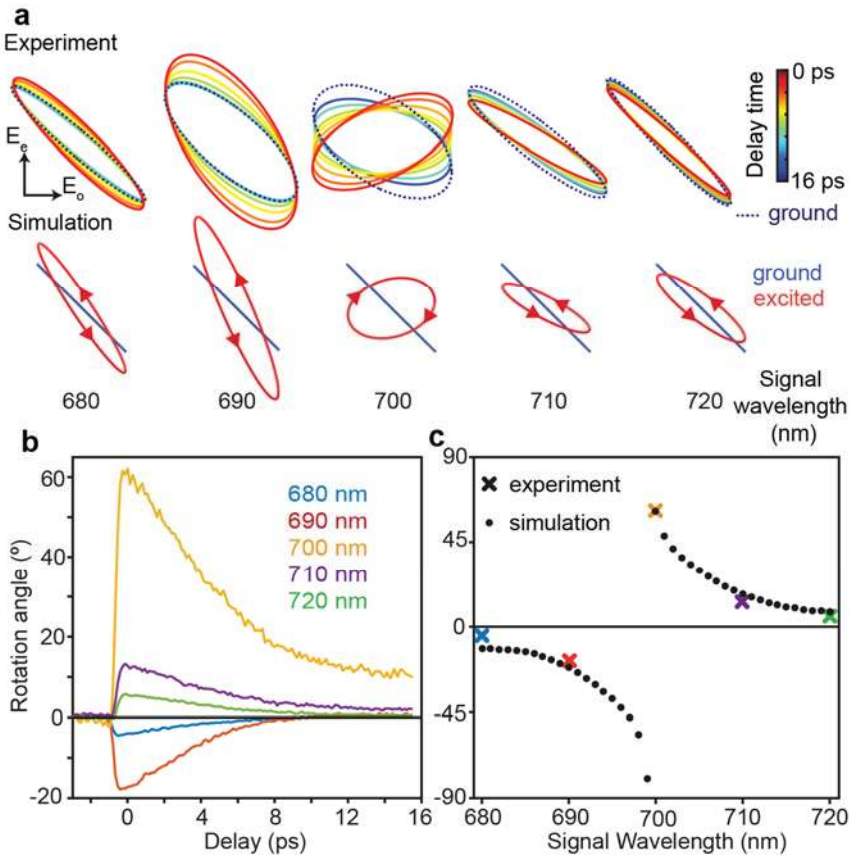

Fig. 3. Dynamics of polarization state of transmitted light. (a) Upper-row: experimental time-dependent polarization state ellipses for the transmitted light. The time-delay between control and signal beams is color-coded. Control light parameters as in (a). The incident light polarization was optimized to minimize the cross-polarized component at each measured wavelength. Lower-row: simulated polarization state of the transmitted light without control light illumination T_e = 300 K (ground state) and under control light illumination T_e = 900 K (excited state). **(b)** The dependence of the induced rotation of the polarization ellipse on time after the excitation. **(c)** Spectral dependence of the maximum polarization rotation angle extracted from (a): (crosses) experiment and (dots) simulation.

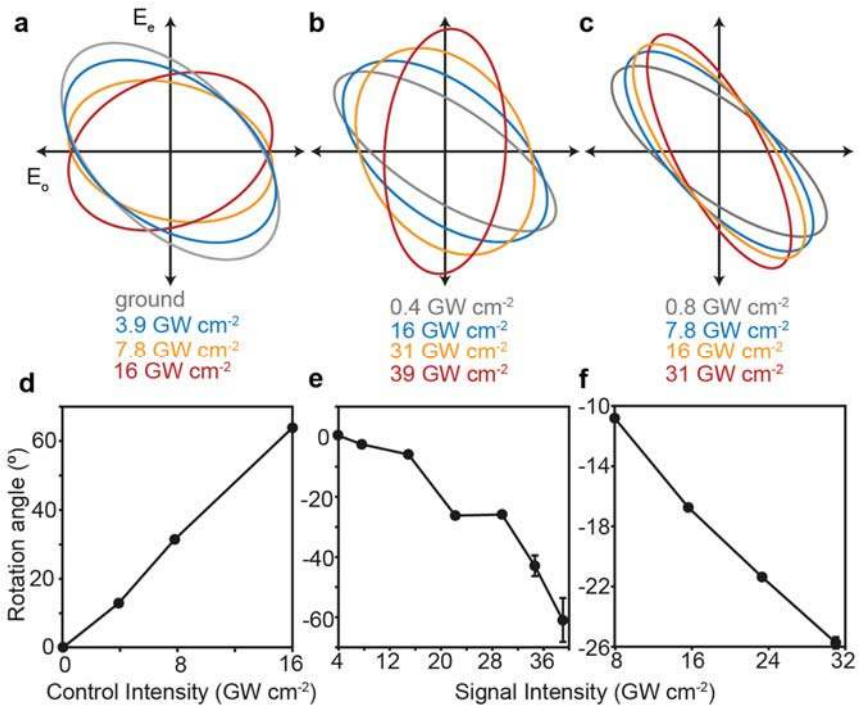

Fig. 4. **Power dependence of polarization switching.** (**a**) Polarization state dependence of the 700 nm signal light on the intensity of the 585 nm control light. (**b, c**) Dependence of the polarization of the transmitted light on the intensity of the incident light for a wavelength (b) 700 nm for the metamaterial as in Fig. 2 with the *e*-wave resonance at 698 nm and (c) 600 nm for the metamaterial with *e*-wave resonance at 590 nm. **(d-f)** The intensity dependence of the polarization ellipse rotation angle from the ground state plotted from a-c, respectively. Intensity of the pulse is given by its peak power density.

Data availability. All data supporting this research are provided in full in the results section and supplementary materials. The data that support the plots within this paper and other findings of this study are available from the corresponding author upon reasonable request.

References

1 Gansel, J. K. *et al.* Gold Helix Photonic Metamaterial as Broadband Circular Polarizer. *Science* **325**, 1513-1515 (2009).

2 Plum, E. *et al.* Metamaterial with negative index due to chirality. *Phys. Rev. B* **79**, 035407 (2009).

3 Ginzburg, P. *et al.* Manipulating polarization of light with ultrathin epsilon-near-zero metamaterials. *Opt. Exp.* **21**, 14907-14917 (2013).

4 Zhao, Y. & Alù, A. Manipulating light polarization with ultrathin plasmonic metasurfaces. *Phys. Rev. B* **84**, 205428 (2011).

5 Mousavi, S. A., Plum, E., Shi, J. H. & Zheludev, N. I. Coherent control of optical polarization effects in metamaterials. *Sci. Rep.* **5**, 8977 (2015).

6 Zhang, S. *et al.* Photoinduced handedness switching in terahertz chiral metamolecules. *Nat. Commun.* **3**, 942 (2012).

7 Kamaraju, N. *et al.* Subcycle control of terahertz waveform polarization using all-optically induced transient metamaterials. *Light Sci. Appl.* **3**, 155 (2014).

8 Poddubny, A., Iorsh, I., Belov, P. & Kivshar, Y. Hyperbolic metamaterials. *Nat. Photon.* **7**, 948-957 (2013).

9 Wurtz, G. A. *et al.* Designed ultrafast optical nonlinearity in a plasmonic nanorod metamaterial enhanced by nonlocality. *Nat. Nano.* **6**, 107-111 (2011).

10 Neira, A. D. *et al.* Eliminating material constraints for nonlinearity with plasmonic metamaterials. *Nat. Commun.* **6** (2015).

11 Schäferling, M., Dregely, D., Hentschel, M. & Giessen, H. Tailoring Enhanced Optical Chirality: Design Principles for Chiral Plasmonic Nanostructures. *Phys. Rev. X* **2**, 031010 (2012).

12 Zhao, R., Zhang, L., Zhou, J., Koschny, T. & Soukoulis, C. M. Conjugated gammadion chiral metamaterial with uniaxial optical activity and negative refractive index. *Phys. Rev. B* **83**, 035105 (2011).

13 Decker, M., Zhao, R., Soukoulis, C. M., Linden, S. & Wegener, M. Twisted split-ring-resonator photonic metamaterial with huge optical activity. *Opt. Lett.* **35**, 1593-1595 (2010).

14 Mousavi, S. A., Plum, E., Shi, J. & Zheludev, N. I. Coherent control of optical polarization effects in metamaterials. *Sci. Rep.* **5**, 8977 (2015).

15 Zhu, H., Yin, X., Chen, L., Zhu, Z. & Li, X. Manipulating light polarizations with a hyperbolic metamaterial waveguide. *Opt. Lett.* **40**, 4595-4598 (2015).

16 Ren, M., Plum, E., Xu, J. & Zheludev, N. I. Giant nonlinear optical activity in a plasmonic metamaterial. *Nat. Commun.* **3**, 833 (2012).

17 Genevet, P. *et al.* Ultra-thin plasmonic optical vortex plate based on phase discontinuities. *Appl. Phys. Lett.* **100**, 013101 (2012).

18 Yu, N. *et al.* A Broadband, Background-Free Quarter-Wave Plate Based on Plasmonic Metasurfaces. *Nano letters* **12**, 6328-6333 (2012).

19 Ding, F., Wang, Z., He, S., Shalaev, V. M. & Kildishev, A. V. Broadband High-Efficiency Half-Wave Plate: A Supercell-Based Plasmonic Metasurface Approach. *ACS nano* **9**, 4111-4119 (2015).

20 Zhu, B. *et al.* Polarization modulation by tunable electromagnetic metamaterial reflector/absorber. *Opt. Exp.* **18**, 23196-23203 (2010).

21 Cui, J. H. *et al.* Dynamical manipulation of electromagnetic polarization using anisotropic meta-mirror. *Sci Rep* **6** (2016).

22 Wang, D. C. *et al.* Switchable Ultrathin Quarter-wave Plate in Terahertz Using Active Phase-change Metasurface. *Sci. Rep.* **5** (2015).

23 Kan, T. *et al.* Enantiomeric switching of chiral metamaterial for terahertz polarization modulation employing vertically deformable MEMS spirals. *Nat. Commun.* **6** (2015).

24 Born, M. & Wolf, E. *Principles of optics : electromagnetic theory of propagation, interference and diffraction of light*. 7th expanded edn, 806-808 (Cambridge University Press, 1999).

25 Vasilantonakis, N., Nasir, M. E., Dickson, W., Wurtz, G. A. & Zayats, A. V. Bulk plasmon-polaritons in hyperbolic nanorod metamaterial waveguides. *Laser Photonics Rev.* **9**, 345-353 (2015).

26 Markowicz, P. P. *et al.* Phase-sensitive time-modulated surface plasmon resonance polarimetry for wide dynamic range biosensing. *Opt. Exp.* **15**, 1745-1754 (2007).

27 Svedendahl, M., Verre, R. & Kall, M. Refractometric biosensing based on optical phase flips in sparse and short-range-ordered nanoplasmonic layers. *Light Sci. Appl.* **3** (2014).

28 Evans, P. *et al.* Growth and properties of gold and nickel nanorods in thin film alumina. *Nanotechnology* **17**, 5746 (2006).

29 Nasir, M. E. *et al.* Tuning the effective plasma frequency of nanorod metamaterials from visible to telecom wavelengths. *Appl. Phys. Lett*. **107** (2015).

30 Lissberg.Ph & Nelson, R. G. Optical-Properties of Thin-Film Au-Mgf2 Cermets. *Thin Solid Films* **21**, 159-172 (1974).

31 Elser, J., Wangberg, R., Podolskiy, V. A. & Narimanov, E. E. Nanowire metamaterials with extreme optical anisotropy. *Appl. Phys. Lett.* **89**, 261102 (2006).

32 Wells, B. M., Zayats, A. V. & Podolskiy, V. A. Nonlocal optics of plasmonic nanowire metamaterials. *Phys. Rev. B* **89**, 035111 (2014).

33 Tsai, K.-T. *et al.* Looking into Meta-Atoms of Plasmonic Nanowire Metamaterial. *Nano letters* **14**, 4971-4976 (2014).

Acknowledgements This work has been supported, in part, by EPSRC (UK) and the ERC iPLASMM project (321268). A.V.Z. acknowledges support from the Royal Society and the Wolfson Foundation. G.A.W. acknowledges support from the EC FP7 project 304179 (Marie Curie Actions). F. J. R.-F. acknowledges financial support from the ERC-2016-StG-714151 PSINFONI project. Data access statement: All data supporting this research are provided in full in the results section and extended data sets.

Author Contributions. L.H.N, F.J.R.F and A.V.Z. developed the idea and designed the experiments. L.H.N., G.A.W and N.O. performed the experiments. L.H.N. and F.J.R.F. performed numerical simulations and data processing. M.E.N and R.M.C.C fabricated the metamaterial samples. L.H.N, F.J.R.F and A.V.Z. wrote the manuscript. All authors commented on the manuscript.

Author Information. Reprints and permissions information is available at www.nature.com/reprints. The authors declare no competing financial interests. Correspondence and requests for information should be addressed to L.H.N (luke.nicholls@kcl.ac.uk).